Computational Study Illustrating NCN-Pincer Palladium(IV) Involvement in Generating Pd^0 Species to Facilitate Pd^0/Pd^{II} Heck-type Catalysis with Diphenyliodine(III) Species

Allan J. Canty* and Alireza Ariafard*

ABSTRACT: Density functional theory has been applied in a mechanistic study of the role of a pincer complex Pd^{II}(NCN-*N,C,N*)(O_2CPh-*O*) ([NCN]- = [2,6-(Me_2NCH_2)$_2C_6H_3$]$^-$) (**3**) in Heck-type catalysis in the presence of diphenyliodine(III) triflate as the oxidative arylating agent for CH_2=CHAr and bicarbonate as the base to afford PhCH=CHAr (Ar = *p*-BrC_6H_4). The initially formed palladium(IV) complex PhPd(NCN-*N,C,N*)(OBz···$HOCO_2$-*O,O*) (**9**) ($\Delta G^{\ddagger}$ 31.6 kcal/mol), undergoes Ph···C_{ipso} reductive elimination to form Pd^{II}{NC(Ph)N-*N,C,N*}(OBz···$HOCO_2$-*O,O*) (**11**) ($\Delta G^{\ddagger}$ 25.6 kcal/mol), which is reduced by bicarbonate to form palladium(0) species. Reduction to Pd^0 occurs via deprotonation of one NMe_2 group by bicarbonate to provide a "-CH_2-N(Me)-CH_2-Pd^{II}" moiety ($\Delta G^{\ddagger}$ 23.6 kcal/mol) followed by nucleophilic attack on this moiety by bicarbonate to give a Pd^0 product with a "-CH_2-NMe(CH_2OCO_2H)" group ($\Delta G^{\ddagger}$ 14.5 kcal/mol). The Pd^0 complex undergoes exceptionally facile oxidative addition by $Ph_2I(HCO_3)$ ($\Delta G^{\ddagger}$ 5.1 kcal/mol). Modelling the Pd^0 complex as [Pd(benzene)(O_2CPh)]$^-$ provides a similar result ($\Delta G^{\ddagger}$ 5.6 kcal/mol), allowing entry to $PhPd^{II}$ species able to undergo migratory insertion for CH_2=CAr ($\Delta G^{\ddagger}$ 14.4 kcal/mol) and β-hydride elimination ($\Delta G^{\ddagger}$ 16.2 kcal/mol) processes of Pd^0/Pd^{II} Heck-type catalysis. Activation barriers for reduction of Pd^{IV} to Pd^0, and in the Heck-type process, are lower than initial oxidation to form Pd^{IV} species, ensuring that only a small quantity of Pd^{II}(NCN)(OBz) (**3**) is consumed, in accord with its presence on completion of catalysis. Computational studies of Pd^{IV}-mediated Heck-type catalysis revealed energetically unfavorable processes, and a preference for formation of CH_2=C(Ar)Ph rather than experimentally reported PhCH=CHAr. This study reveals the role of a pincer complex as a precatalyst, oxidation of Pd^{II} to Pd^{IV} followed by reductive elimination, the role of bicarbonate in reducing Pd^{II} to Pd^0, extremely facile oxidative addition of a diaryliodine(III) reagent to Pd^0, and selectivity differences in migratory insertion for Pd^{II} and Pd^{IV} centers.

KEYWORDS: Heck-type catalysis, DFT mechanism, palladium(IV), pincer precatalyst, hypervalent iodine(III) oxidant, bicarbonate reductant

INTRODUCTION

The Heck reaction occupies a central role in modern organic synthesis.[1] Originally developed as a process for the arylation of alkenes with arylmercury compounds,[2] its extension[3a-c] to include transfer from aryl iodides has transformed synthetic routes for substitution of alkenes (often termed Mizoroki-Heck reaction), including vinyl transfer.[4] The general "textbook" catalytic cycle for application with organic halides, illustrated in Scheme 1a, is applicable for a wide range of reagents capable of facilitating the initial oxidative addition to Pd^0, including X in ArX as chloride[5] and triflate.[6] Upon oxidative addition, a *syn*-insertion reaction at a Pd^{II} center is followed by rotation about the C-C bond to facilitate β-hydride elimination, and reaction with base to remove hydride with concomitant reduction of Pd^{II} to Pd^0.

Diaryliodine(III) reagents Ar_2IX are also able to participate in Heck-type reactivity in organic solvents,[7,8] at temperatures that are very mild for Heck reactions, including room temperature[8a,b] and 50 °C.[8c] In a related manner diarylodonium reagents also support aryl transfer reactions for heteroarenes.[9] Extensive experimental evidence[10a,11a,12a] and computational studies[10b,11b,12b] support roles for diorganoiodine(III) reagents facilitating synthesis involving participation of oxidation states higher than +II for Pd: Pd^{II}/Pd^{III} [10b] and Pd^{II}/Pd^{IV} cycles,[11] and the Pd^{IV} mediated stoichiometric synthesis of benzofurans.[12] In this context, we noted with interest the application of a Pd^{II}-pincer complex **3** (5 mol %) for the reaction illustrated in Scheme 1b,[8c] as **3** is known to react with a related iodine(III) reagent, (Me_3SiCC)PhI(OTf), to form the alkynylpalladium(IV) complex Pd(OBz)(OTf)($CCSiMe_3$)(NCN).[13] In a comprehensive review of the application of pincer ligands in Heck catalysis, Selander and Szabó examine the feasibility of Pd^{II}/Pd^{IV} cycles, including for catalysis involving **3** and

diaryliodine(III) reagents at 50 °C, and reduction to Pd^0 as a characteristic feature of high temperature Heck reactions (typically >100 °C).[7c,14]

Scheme 1. (a) Simplified Schematic of the Heck Reaction, Showing Only the Organic Ligands in Pd^{II} Intermediates, (b) a Heck-type Reaction Employing a Pincer-Pd^{II} Complex[8c] that is Examined Herein by Computational Methods, (c) a Pd^{II}/Pd^{IV} Model Directly Analogous to the Pd^0/Pd^{II} Cycle in (a), and (d) Computational Study of the Reaction of 3 with $Ph_2I(OTf)$ in the Presence of Bicarbonate[15]

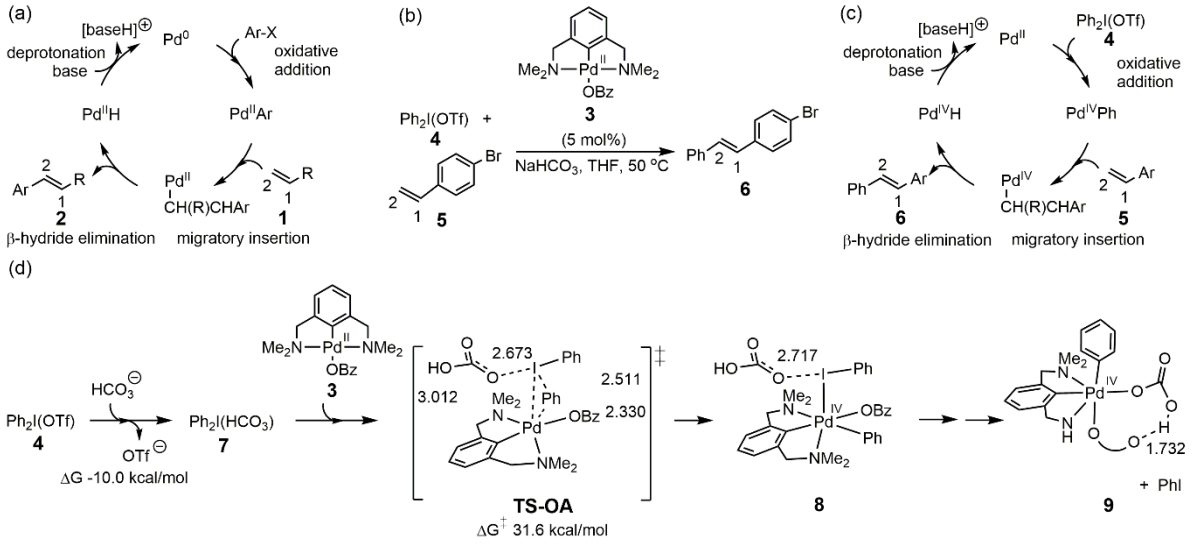

Experimental data for the reaction in Scheme 1b, extended to include alkenes with OMe or $SiMe_2Ph$ in place of Br, and related PCP-pincers, are consistent with catalytic Pd^{IV} involvement,[8c] e.g. via the process illustrated in Scheme 1c as an analog of Scheme 1a but, as noted,[7c,8c] the evidence is insufficient to definitely confirm the cycle. For reactions employing **3** [8c,d] and the related complex $Pd(PCP)(O_2CCF_3)$ (PCP = $[2,6\text{-}(Ph_2PO)_2C_6H_3\text{-}P,C,P]^-$),[8c] unreacted complex is detected at the completion of reaction and a mercury drop test supports the absence of Pd^0 in catalysis. In view of the wide utility of this synthesis of alkenes in high yields,[8c] we have undertaken a density functional theory (DFT) examination of mechanism for one of the reactions studied experimentally (Scheme 1b), with the aim of determining the role of **3**. This investigation follows our computational study of the reaction of **3** with diphenyliodonium triflate (**4**) in the presence of bicarbonate to form $PhPd^{IV}(NCN)(OBz\cdots HCO_3)$ (**9**) (Scheme 1d).[15]

Results herein indicate that oxidation of the pincer-Pd^{II} complex **3** to form Pd^{IV} complex **9** (Scheme 1c)[15] leads to Ph-pincer reductive elimination from **9** followed by reduction of the resulting Pd^{II} complex facilitated by bicarbonate to generate Pd^0 species. Palladium(0) undergoes extremely facile oxidative addition with $Ph_2I(HCO_3)$ to form phenylpalladium(II) species. Computation for a model complex shows that $PhPd^{II}$ species in the reported reaction conditions can participate in reaction with an alkene, such that facile Heck-type Pd^0/Pd^{II} catalysis is operative. This study reveals the role of a pincer-Pd^{II} complex as a precatalyst, the role of bicarbonate in reducing Pd^{II} to Pd^0, extremely facile oxidative addition by a diaryliodine(III) reagent to Pd^0, and different preferences for migratory insertion at Pd^{II} and Pd^{IV} centers.

EXPERIMENTAL DETAILS

Computation was carried out in an identical manner to that used for the oxidation of **3** (Scheme 1d).[15] Gaussian 16[16] was used to fully optimize all structures at the M06 level of theory.[17] For all calculations, solvent effects were considered using the SMD solvation model[18] with tetrahydrofuran as the solvent in view of its application in catalysis (Scheme 1b).[8c] The SDD basis set[19] with effective core potential (ECP*)* was chosen to describe palladium and iodine. The 6-31G(d) basis set was used for other atoms. This basis set combination will be referred to as BS1. Frequency calculations were carried out at the same level of theory as those for the structural optimization. Computation included application of the ultrafine grid as the default in Gaussian 16. Transition structures were located using the Berny algorithm, contained one imaginary frequency, and exhibited atom

displacements consistent with the anticipated reaction pathway. The nature of the transition structures was confirmed from the potential energy surface scans. Precursors to and products from transition states were obtained by optimizations after small displacements in the direction of the normal mode corresponding to the imaginary frequency. To further refine the energies obtained from the SMD/M06/BS1 calculations, we carried out single-point energy calculations in tetrahydrofuran using the M06 functional method,[16] incorporating Grimme's D3 computation to account more completely for dispersion,[20] for all of the structures with a larger basis set (BS2). BS2 utilizes the def2-TZVP basis set[21] on all atoms with an effective core potential including scalar relativistic effect for palladium and iodine. An additional correction for the compression of 1 mol of an ideal gas from 1 atm to the 1 M solution phase standard state (1.89 kcal mol^{-1})[22] was applied.

RESULTS AND DISCUSSION

Heck-type Reaction at a Pd^{IV} Center. Reaction of the pincer-Pd^{IV} complex **9** with alkenes in a Heck-type manner requires coordination of the alkene to the palladium center followed by a key transition state for migratory insertion (Scheme 1c). This step would constitute, in this system, the minimum barrier for the overall Heck-type process commencing from **9**. Computation was explored for feasible transition states that could lead to formation of the experimentally formed *syn*-product (**6**) obtained using CH_2=CHAr (Ar = *p*-bromophenyl) as a representative alkene reagent (Scheme 2, in black),[8c] and also explored for the alternative unobserved product, CH_2=C(Ar)Ph (**10**) (in blue). Scheme 2 illustrates eight of ten transition states identified by computation, together with precursors **prec-TS$_{2/1}$** and **prec-TS$_{1/2}$** for the lowest energy transition states (to the left of complex **9**), and the profile for reductive elimination from **9** (to the right of **9**, discussed in a later Section).[23]

Scheme 2. Energy Profile for C···C Reductive Elimination from the Pincer-Pd^{IV} Complex 9, and Transition States Explored for the Migratory Insertion Step in a Heck-type Mechanism, together with the Precursor Adducts for Transition States TS$_{2/1}$ and TS$_{1/2}$, and Reductive Elimination from 9. Selected Interatomic Distances (Å) are shown, and Energies ΔG (ΔH) are in kcal/mol Relative to 9

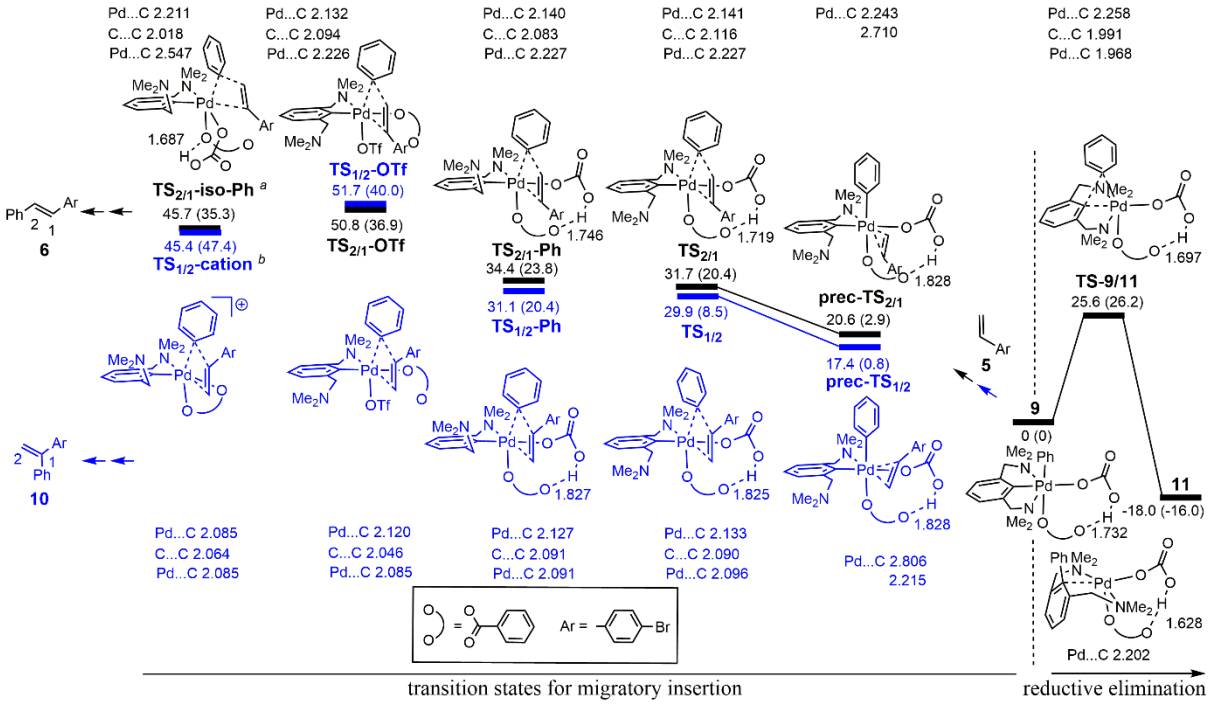

[a] **TS2/1-iso** has ΔG (ΔH) 45.8 (34.9) kcal/mol. [b] **TS2/1-cation** has ΔG (ΔH) 45.9 (46.7) kcal/mol.

The model transition states utilized one uncoordinated pincer arm to permit interaction of the alkene with palladium. Conformations were examined with this arm adjacent to the phenyl group, e.g. **TS$_{2/1}$-Ph**, or on the opposite side of the pincer arene plane, e.g. **TS$_{2/1}$**. The immediate precursor Pd^{IV}(η^2-alkene) species, illustrated for **prec-TS$_{2/1}$** and **prec-TS$_{1/2}$**, and product Pd^{IV}-alkyl species were confirmed by intrinsic reaction coordinate (IRC) computation. A transition state with the bicarbonate group adjacent to the uncoordinated arm (**TS$_{2/1}$-iso-Ph**) is significantly higher in energy ($\Delta\Delta G^{\ddagger}$ > 11.0 kcal/mol) than analogs with the alkene group adjacent to the uncoordinated arm (**TS$_{2/1}$-Ph**, **TS$_{2/1}$**, **TS$_{1/2}$-Ph**, **TS$_{1/2}$**). High barriers are also found for triflate as the ancillary

ligand (**TS$_{1/2}$-OTf**. **TS$_{2/1}$-OTf**), and on removal of bicarbonate to form cationic transition states (**TS$_{1/2}$-cation-Ph** illustrated, **TS$_{2/1}$-cation** in footnote b).

Transition states in which the pendant NMe_2 group is adjacent to the phenyl group (**TS$_{2/1}$-Ph**, **TS$_{1/2}$-Ph**) compute as higher energy than those with the pendant group well removed from the site of migratory insertion (**TS$_{2/1}$**, **TS$_{1/2}$**).

For the four lower energy transition states, we find that those leading to the observed product PhCH=CHAr (**6**) are disfavored compared with the unobserved product CH_2=C(Ar)Ph (**10**). This result is in marked contrast to migratory insertion at a Pd^{II} center,[1] for which the observed product is computed as favored by 3.5 kcal/mol in the present system (see later Section). We attribute the preference for formation of the unobserved product at a Pd^{IV} center to an electronic effect related to the ability of the arene group to delocalize positive charge in the formal Pd^{II} resonance representations for the precursor alkene adduct (Scheme 3b, in blue). The high formal oxidation state Pd^{IV} enhances the role of Pd^{II} resonance forms which can be more readily accommodated by delocalization compared with the alternative form '$Pd^{(-)}$-CH(Ar)-$CH_2^{(+)}$' illustrated in Scheme 3a.

These observations, taken together with the preference for reductive elimination, $\Delta\Delta G^{\ddagger}$ -6.1 kcal/mol for **TS-9/11** relative to **TS$_{2/1}$** (Scheme 2), indicate against a mechanism involving migratory insertion at a Pd^{IV} center.

Scheme 3. Representative Resonance Structures for the Precursor Adducts leading to (a) PhCH=CHAr (6), and (b) the Unobserved Product CH_2=C(Ar)Ph (10), in blue

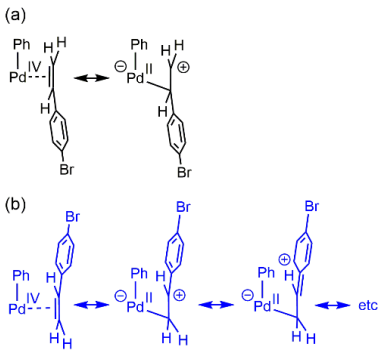

Exploration of the Reactivity of Pincer-Pd^{II} Complex Pd(NCN)(OBz) (3) with Alkene Followed by Oxidation. In searching for other mechanisms that may involve Pd^{IV} species with **3** as a catalyst, we considered the possibility of processes that are the reverse of the above approach, i.e. activation of the alkene by the pincer-Pd^{II} complex **3** followed by oxidative arylation leading to C···C reductive elimination at a Pd^{IV} center. We explored two mechanisms, and both were found to require very high energy transition states: (i) formation of *trans*-Pd^{II}(NCN)(CH=CHAr) (*trans*-disposed PdC_2) via CH-activation employing the benzoate group ($\Delta G^{\ddagger}$ 38.3 kcal/mol) followed by oxidative addition of $Ph_2I(HCO_3)$ ($\Delta G^{\ddagger}$ 53.8 kcal/mol), and (ii) bicarbonate assisted deprotonation of a coordinated alkene to form *cis*-Pd^{II}(NCN)(CH=CHAr)(OBz)]$^-$ ($\Delta G^{\ddagger}$ 34.7 kcal/mol) followed by oxidation ($\Delta G^{\ddagger}$ 48.0 kcal/mol) (Schemes S1 and S2 in the Supporting Information).

Thus, we are led to the conclusion that the *catalytic cycle* in this system does not involve Pd^{IV} in Heck-type migratory insertion, or related processes involving alkene activation followed by oxidation of a Pd^{II} center to Pd^{IV}.

Reductive Elimination from the Pd^{IV} Complex PhPd(NCN-*N,C,N*)(OBz···$HOCO_2$-*O,O*) (9) and Reduction of Pd^{II} to Pd^0. As discussed above, reductive elimination via **TS-9/11** to give **11** ($\Delta G^{\ddagger}$ 25.6 kcal/mol) occurs with a lower barrier than that for migratory insertion at a Pd^{IV} center (Scheme 2).

Reduction of Pd^{IV} to Pd^{II} encouraged us to examine further reduction to Pd^0. Amines are known to reduce Pd^{II} complexes,[24] including from detailed spectroscopic studies of reduction of SCS- and PCP-pincer complexes.[14c] The bicarbonate base for Heck reactions has also been mentioned as a potential reductant.[24] We found that NMe deprotonation of a pincer arm by bicarbonate provides an initial step (**12** → **13** in Scheme 4) toward reduction.[24] During examination of other options we found that the pincer in **11** would not facilitate deprotonation of the -CH_2- moiety, but does allow bicarbonate to form adduct **12** via interaction of an NMe group. A transition state for deprotonation (**TS-12/13**) gives **13**, and H_2CO_3 departs to give **14**. Reaction of **14** with a second bicarbonate, by nucleophilic attack at carbon of the $PdCH_2$ group (**TS-15/16**), gives the Pd^0

complex **16**. Structure **16** exhibits a linear "(η^2-arene)Pd^0(OBz)" moiety. Ligand exchange to form an analogous "(N-donor)Pd(OBz)" moiety in **17** is endergonic.

Of particular note, the barriers for deprotonation ($\Delta G^{\ddagger}$ 23.6 kcal/mol) and reduction ($\Delta G^{\ddagger}$ 14.5 kcal/mol) are lower than that for the initial reductive elimination at Pd^{IV} in **9** ($\Delta G^{\ddagger}$ 25.6 kcal/mol), and the process to form the Pd^0 product **16** is exergonic.

The overall reaction of deprotonation followed by reduction is summarized in Scheme 5a. The N···C and Pd···C interactions for **13-15** are shown in red in Schemes 4 and 5. Resonance structures for intermediates **13-15** (Scheme 5b) illustrate partial formal reduction on deprotonation. In accord with the resonance analysis proposing partial multiple bond character for the imine group, the N-CH_2 distances (1.379-1.403 Å) are shorter than the single bond N-Me distances for NMe_2 groups in these structures (1.460 Å).

Scheme 4. Computed Energy Profile for Reductive Elimination by Pd^{IV} Complex 9, Followed by Reduction by Bicarbonate to give Pd^0 Complex 16 and Depiction of Structures for TS-9/11, TS-12/13 and TS-15/16. Selected Interatomic Distances (Å) are shown, and Energies ΔG (ΔH) are in kcal/mol relative to 9.

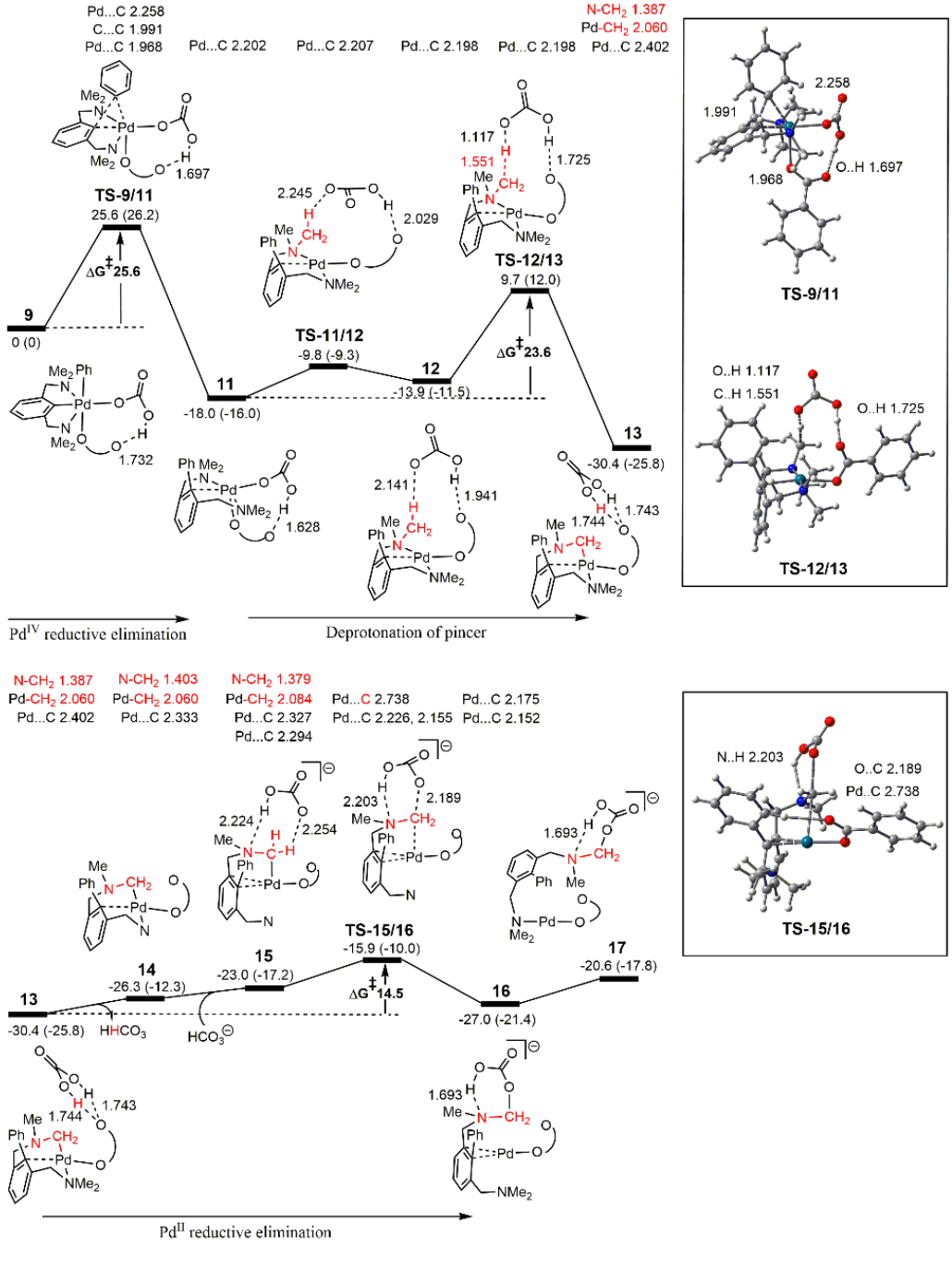

Scheme 5. Schematics for Bonding in Key Moieties for (a) Overall Reaction in Reduction of Pd^{II} to Pd^0, and (b) Resonance for Intermediates in the Reduction Process

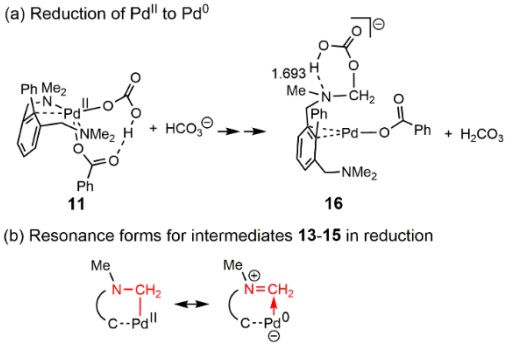

Heck-type Reaction for Pd^0 Utilizing $Ph_2I(HCO_3)$ as the Arylating Agent. We are unaware of any computational studies of oxidative transfer to Pd^0 by diorganoiodine(III) reagents, and thus we have explored this reaction using $[Pd(benzene)(O_2CPh)]^-$ (**18**) as a model for Pd^0 species such as **16** in Scheme 4. We found that $Ph_2I(HCO_3)$ forms adduct **19**, leading to **TS-19/20** and immediate product **20** (Scheme 6). Departure of bicarbonate from **20** provides **21**. A similar process has been computed for the reaction of $Ph_2I(HCO_3)$ with the product **16**, shown in Scheme S3 in the Supporting Information.

Scheme 6. Computed Energy Profile for the Reaction of $Ph_2I(HCO_3)$ (7) with $[Pd(benzene)(O_2CPh)]^-$ (18) as a Model for Pd^0 Intermediates. Selected Interatomic Distances (Å) are shown, and Energies ΔG (ΔH) are in kcal/mol Relative to 18

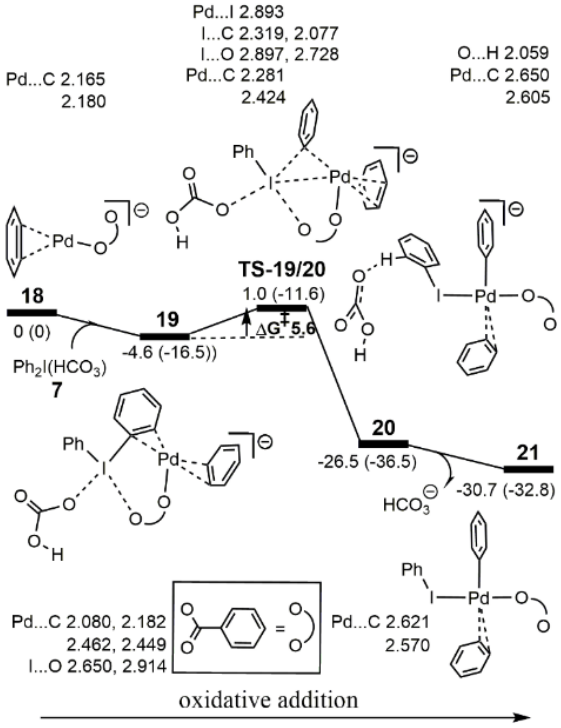

A significant feature of the reaction illustrated in Scheme 6, and for the reaction of **16**, is the very low barrier for oxidative addition ($\Delta G^{\ddagger}$ 5.6 kcal/mol for **18**, 5.1 kcal/mol for **16**). This step has the lowest barrier for the entire system, including for the completion of the $Pd^{0/II}$ Heck-type reaction (see below). These observations illustrate that, if any Pd^0 is formed from **3** (added at 5 mol %) in the presence of stoichiometric $Ph_2I(HCO_3)$ (Scheme 1b), it would be immediately oxidized to Pd^{II}.

Computation for completion of the reaction is shown in Scheme 7, using the general Heck manifold[27] for guidance. Ligand exchange for **21** gives an alkene complex **22**, which reacts exergonically with bicarbonate to form **23** exhibiting a coordinated [benzoate···bicarbonate]$^-$ ligand analogous to that noted above for Pd^{IV} species. Complex **23** undergoes migratory insertion via **TS-23/24** to give **24**. Facile rotation about Pd-C_γ in **24** provides **25** with a geometry suitable for β-hydride elimination via **TS-25/26** to form the Pd^{II}(hydride)(alkene) structure **26**.

Scheme 7. Completion of the Heck-type Reaction Following Oxidative Arylation of the Pd^0 Model (Scheme 6). Stationary Points Leading to the Experimentally Unobserved Product are shown in color. Selected Interatomic Distances (Å) are shown, and Energies ΔG (ΔH) are in kcal/mol Relative to the Pd^0 Complex [Pd(benzene)(O_2CPh)]$^-$ (18) used as a Model for Pd^0/Pd^{II} Catalysis.

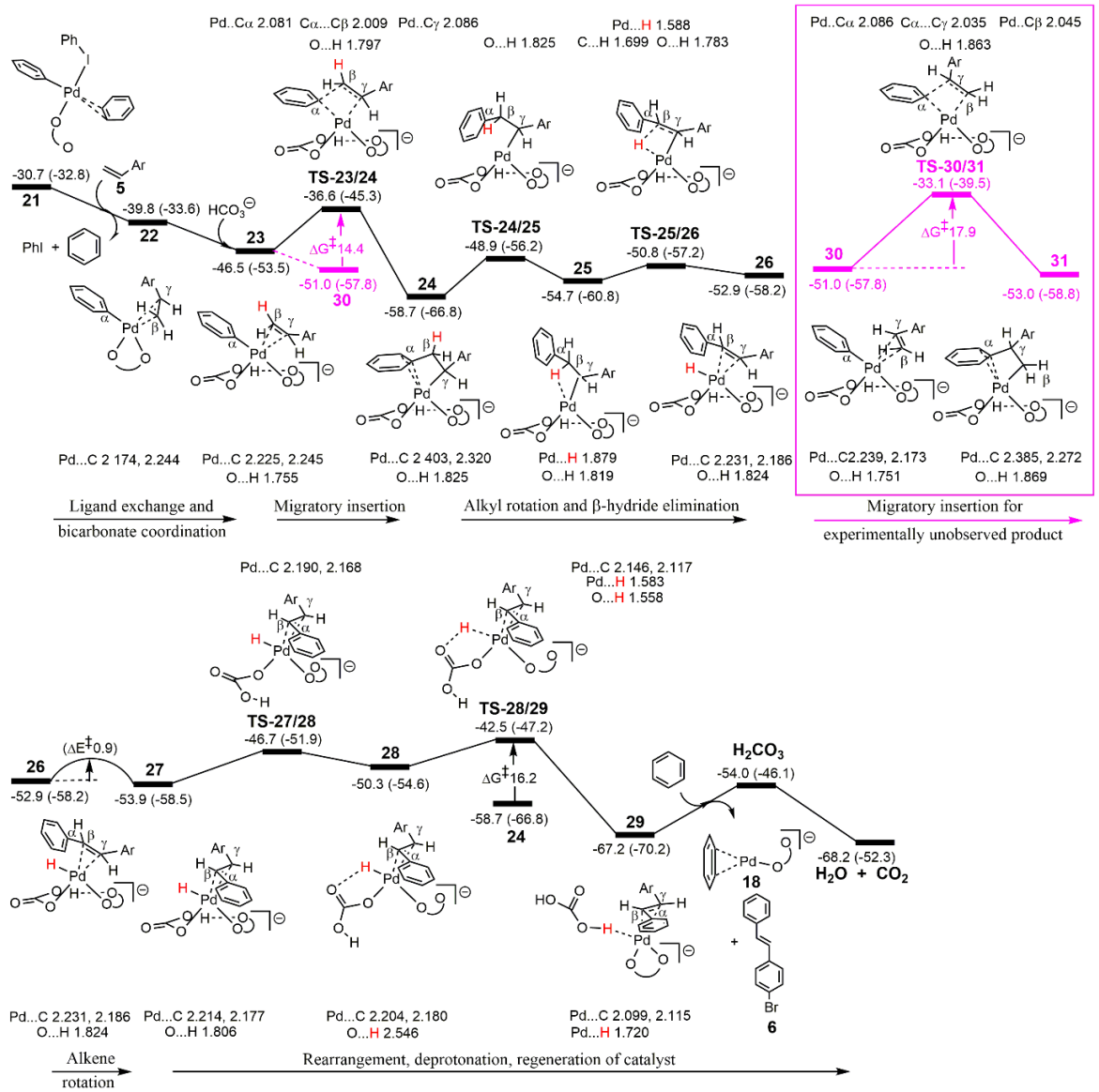

A low barrier for alkene rotation in **26** allows entry to the process of deprotonation enabled by coordinated bicarbonate via transition states **TS-27/28** and **TS-28/29** to give the product alkene coordinated to Pd^0 in **29**. Ligand exchange and dissociation of carbonic acid provides the experimentally observed alkene product (**6**). Computation for the unobserved isomer, CH_2=C(Ar)Ph (**10**), via the rate-limiting migratory insertion step **TS-30/31** (in color, Scheme 7), reveals that this process is uncompetitive against **TS-23/24** ($\Delta\Delta G^‡$ 3.5 kcal/mol).

CONCLUSIONS

The DFT results lead us to conclude that the initial oxidative addition to form a Pd^{IV} complex is followed by reductive elimination to Pd^{II}, and then further reduction to Pd^0 followed by Pd^0/Pd^{II} catalysis (Scheme 8).

Scheme 8. Mechanism Illustrating (a) Oxidative Arylation of the Precatalyst 3 Followed by Reductive Elimination, (b) Reaction with Bicarbonate to Generate Pd^0 Species, and (c) Model for Heck-type Pd^0/Pd^{II} Catalysis

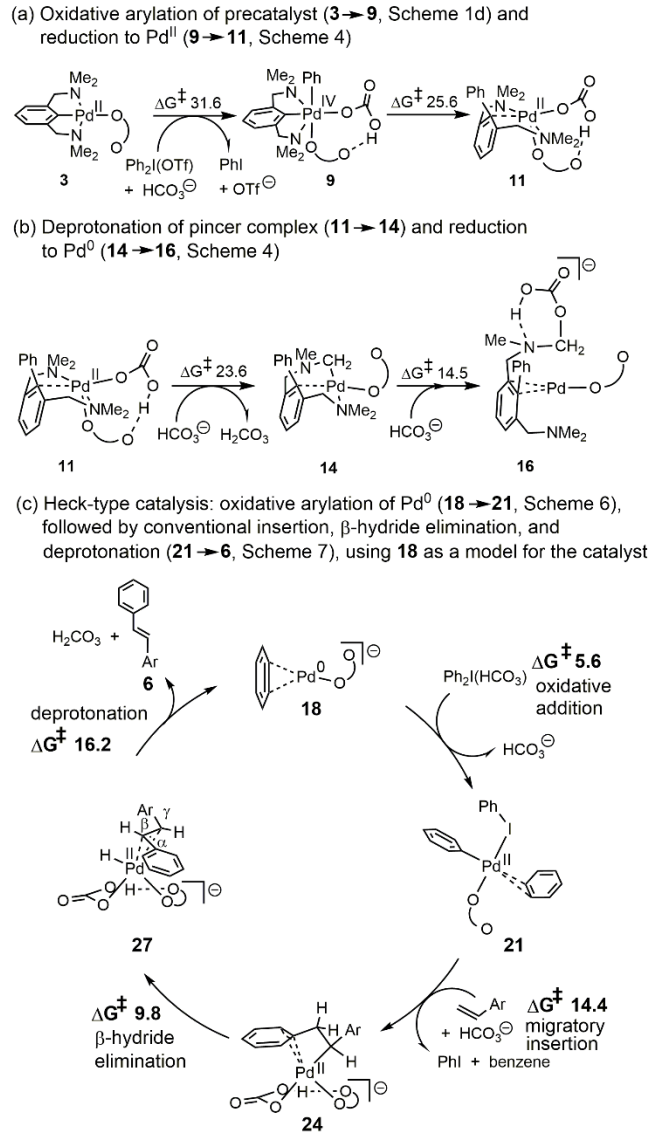

It is notable that the initial oxidative addition of $Ph_2I(HCO_3)$ to Pd^{II}(NCN)(OBz) (**3**) exhibits the highest barrier in the entire system ($\Delta G^{\ddagger}$ 31.6 kcal/mol) (Scheme 8a).[14] Subsequent reductive elimination to give Pd^{II} (**11**) ($\Delta G^{\ddagger}$ 25.6 kcal/mol, Scheme 8a), and Pd^0 (**16**) ($\Delta G^{\ddagger}$ 23.6 kcal/mol, Scheme 8b) allows entry to Heck-type catalysis. For the model Pd^0/Pd^{II} system examined (Scheme 8c), the catalysis has even lower barriers than all prior processes: oxidative addition ($\Delta G^{\ddagger}$ 5.6 kcal/mol), migratory insertion ($\Delta G^{\ddagger}$ 14.4 kcal/mol), β-hydride elimination ($\Delta G^{\ddagger}$ 9.8 kcal/mol), and deprotonation of a hydridopalladium(II) intermediate to regenerate Pd^0 ($\Delta G^{\ddagger}$ 16.2 kcal/mol).

Thus, after a small amount of the pincer precatalyst **3** is reduced to Pd^0, extremely facile oxidative addition to Pd^0 ensuring absence of formation of Pd black,[8c] is followed by facile reaction to give the alkene product and

regenerate Pd^0. This allows experimental identification of the pincer precatalyst **3** at the end of catalysis,[8c] as only a small amount of **3** is consumed.

How does this outcome fit with previous computational work on diorganoiodine(III)/palladium mediated or catalytic systems? We are aware of only three computational reports indicating roles for oxidation states >II for palladium in catalytic cycles or in a stoichiometric reaction involving diorganoiodine(III) reagents: binuclear Pd^{II}/Pd^{III} catalysis utilizing $Ph_2I(BF_4)$ with oxidation of Pd^{II} as the rate-limiting step,[10b] mononuclear Pd^{II}/Pd^{IV} catalysis utilizing $Mes(CF_3CH_2)I(OTf)$ in $alkyl^+$ transfer,[11b] and a Pd^{II}/Pd^{IV} stoichiometric synthesis of benzofurans utilizing $Ph(MeCH{=}CH)I(BF_4)$ in $alkenyl^+$ transfer.[12b] The current study, limited to the NCN-pincer complex Pd^{II}(NCN-*N,C,N*)(O_2CPh-*O*) ([NCN]- = [2,6-$(Me_2NCH_2)_2C_6H_3]^-$) (**3**), illustrates the role of a NCN-pincer-Pd^{II} complex as a *precatalyst that forms the active Pd^0 catalyst after formation of a Pd^{IV} intermediate*. Computation herein reveals new mechanisms for (a) an NMe deprotonation reaction of a coordinated pincer ligand in a Pd^{II} complex by bicarbonate, (b) reduction of Pd^{II} to Pd^0 involving (a) followed by bicarbonate attack on an organic ligand, and (c) extremely facile oxidative addition of $Ph_2I(HCO_3)$ in Heck-type catalysis for arylation of alkenes. We note also several significant roles for bicarbonate, in oxidation and reduction processes, and as a ligand linked with a carboxylate group in Heck-type catalysis.

The examination of reactivity in the NCN-pincer-$Pd^{II/IV}$ system herein indicates that, in particular for d^6, d^8 and pincer systems, consideration of mechanism in catalysis potentially involving oxidative processes at metal centers should include the possibility that pincer complexes can act as precatalysts via preliminary oxidation and subsequent reduction and the operation of lower oxidation state catalysis.

ASSOCIATED CONTENT

Supporting Information

The Supporting Information is available free of charge at https://.....

Energy data, energy profiles, and Cartesian coordinates for calculated structures (PDF)

AUTHOR INFORMATION

Corresponding Author

Allan J. Canty – School of Natural Sciences-Chemistry, University of Tasmania, Hobart, Tasmania 7001, Australia; orcid.org/0000-0003-4091-6040; Email: allan.canty@utas.edu.au

Authors

Alireza Ariafard - School of Natural Sciences-Chemistry, University of Tasmania, Hobart, Tasmania 7001, Australia; orcid.org/0000-0003-2383-6380; Email: alireza.ariafard@utas.edu.au

Complete contact information is available at: https://.....

ACKNOWLEDGMENTS

We acknowledge support from the Australian Research Council and the Australian National Computing Infrastructure.

REFERENCES

(1) Reviews: (a) de Meijere, A.; Meyer, F.E. Fine Feathers Make Fine Birds: The Heck Reaction in Modern Garb. *Angew. Chem. Int. Ed*. **1994**, *33*, 2379. (b) Overman, L. E. Application of Intramolecular Heck Reactions for Forming Congested Quaternary Carbon Centers in Complex Molecule Total Synthesis. *Pure Appl. Chem*. **1994**, *66*, 1423. (c) Cabri, W.; Candiani, I. Recent Developments and New Perspectives in the Heck Reaction. *Acc. Chem. Rev*. **1995**, *28*, 2. (d) Crisp, G. T. Variation on a Theme – Recent Developments on the Mechanism of the Heck Reaction and Their Implications for Synthesis. *Chem. Soc. Rev*. **1998**, *27*, 427. (e) Beletskaya, I. P.; Cheprakov, A. V. The Heck Reaction as a Sharpening Stone of Palladium Catalysis. *Chem. Rev*. **2000**, *100*, 3009. (f) Amatore, C.; Jutand, A. Anionic Pd(0) and Pd(II) Intermediates in Palladium-Catalyzed Heck and Cross-Couling Reactions. *Acc. Chem. Res*. **2000**, *33*, 314. (g) Dounay, A.; Overman, L. The Asymmetric Intramolecular Heck Reaction in Natural Product Total Synthesis. *Chem. Rev*. **2003**, *103*, 2945. (h) Knowles, J. P.; Whiting, A. The Heck-Mizoroki Cross-Coupling Reaction: A Mechanistic Perspective. *Org. Biomol. Chem*. **2007**, *5*, 31. (h) McCartney, D.; Guiry, P. J. The Asymmetric Heck and Related Reactions. *Chem. Soc. Rev*. **2011**, *40*, 5122. (i) Le Bras, J.; Muzart, J. Intermolecular Dehydrogenative Heck Reactions. *Chem. Rev*. **2011**, *111*, 1370. (j) Ruan, J.; Xiao, J. From α-Arylation of

Olefins to Acylation with Aldehydes: A Journey in Regiocontrol of the Heck reaction. *Acc. Chem. Res*. **2011**, *44*, 614. (k) Jagtap, S. Heck Reaction – State of the Art. *Catalysts*, **2017**, *7*, 267.

(2) Heck, R. F. Allylation of Aromatic Compounds with Organopalladium Salts. *J. Am. Chem. Soc*. **1968**, *90*, 5531.

(3) (a) Mizoroki, T.; Mori, K.; Ozaki, A. Arylation of olefin with aryl iodide catalyzed by palladium. *Bull. Chem. Soc. Jpn*. **1971**, *44*, 581. (b) Heck, R. F.; Nolley, J. P. Palladium-Catalyzed Vinylic Hydrogen Substitution Reactions with Aryl, Benzyl. and Styryl Halides. *J. Org. Chem*. **1972**, *37*, 2320. (c) Julia, M.; Duteil, M. Condensation of Aromatic Halides with Olefins, Catalyzed by Palladium. *Bull. Soc. Chim. Fr*. **1973**, 2790.

(4) Jeffery, T. Palladium-Catalysed Vinylation of Organic Halides under Solid-Liquid Phase Transfer Conditions. *J. Chem. Soc., Chem. Commun*. **1984**, 1287.

(5) Ben-David, Y.; Portnoy, M.; Gozin, M.; Milstein, D. Palladium-Catalyzed Vinylation of Aryl Chlorides. Chelate Effect in Catalysis. *Organometallics* **1992**, *11*, 1995.

(6) Jutand, A. Mosleh, A. Rate and Mechanism of Oxidative Addition of Aryl Triflates to Zerovalent Palladium Complexes. Evidence for the Formation of Cationic (σ-Aryl)palladium Complexes. *Organometallics* **1995**, *14*, 1810.

(7) Reviews: (a) Deprez, N. R.; Sanford, M. S. Reactions of Hypervalent Iodine Reagents with Palladium: Mechanisms and Applications in Organic Synthesis. *Inorg. Chem*. **2007**, *46*, 1924. (b) Canty, A. J.; Rodemann, T.; Ryan, J. R. Transition Metal Organometallic Synthesis Utilising Diorganoiodine(III) Reagents. *Adv. Organomet. Chem*. **2008**, *55*, 279. (c) Selander, N.; Szabó, K. J. Catalysis by Palladium Pincer Complexes. *Chem. Rev*. **2011**, *111*, 2048.

(8) (a) Moriarty, R. W.; Epa, W. R.; Awasthi, A. K. Palladium-Catalyzed Coupling of Alkenyl Iodonium Salts with Olefins: A Mild and Stereoselective Heck-Type Reaction Using Hypervalent Iodine. *J. Am. Chem. Soc*. **1991**, *113*, 6315. (b) Kang, S.-K.; Lee, H.-W.; Jang, S.-B.; Kim, T.-H.; Pyun, S.-J. Complete Regioselection in Palladium-Catalyzed Arylation and Alkenylation of Allylic Alcohols with Hypervalent Iodonium Salts. *J. Org. Chem*. **1996**, *61*, 2604. (c) Aydin, J.; Larsson, J. M.; Selander, S.; Szabó, K. J. Pincer Complex-Catalyzed Redox Coupling of Alkenes with Iodonium Salts via Presumed Palladium(IV) Intermediates. *Org. Lett*., **2009**, *11*, 2852. (d) Szabó, K. J. Mechanism of the Oxidative Addition of Hypervalent Iodonium Salts to Palladium(II) Pincer-complexes. *J. Mol. Catal. A: Chemical* **2010**, *324*, 56. (e) Reddy Vaddula, B.; Saha, A.; Leazer, J.; Varma, R. S. A Simple and Facile Heck-Type Arylation of Alkenes with Diaryliodonium Salts Using Magnetically Recoverable Pd-catalyst. *Green Chem*., **2012**, *14*, 2133. (f) Li, J.; Liu, L.; Zhou, Y.-Y.; Xu, S.-Nan, Palladium-Catalyzed Heck-Type Arylation of Acrylate with Diaryliodonium Salts. *RSC Advances*, **2012**, *2*, 3207. (g) Lei, L.; Zou, P.-S.; Wang, Z.-X.; Liang, C.; Hou, C.; Mo, D.-L. Palladacycle-Catalyzed Regioselective Heck Reaction Using Diaryliodonium Triflates and Aryl Iodides. *Org. Lett*. **2022**, *24*, 663.

(9) (a) Deprez, N. R.; Kalyani, D.; Krause, A.; Sanford, M. S. Room Temperature Palladium-Catalyzed 2-Arylation of Indoles. *J. Am. Chem. Soc*. **2006**, *128*, 4972. (b) Pacheco-Benichou, A.; Besson, T.; Fruit, C. Diaryliodonium Salts as Coupling Partners for Transition-Metal Catalyzed C- and N-Arylation of Heteroarenes. *Catalysts*, **2020**, *10*, 483.

(10) (a) Deprez, N.R.; Sanford, M. S. Synthetic and Mechanistic Studies of Pd-Catalyzed C-H Arylation with Diaryliodonium Salts: Evidence for a Bimetallic High Oxidation State Pd Intermediate. *J. Am. Chem. Soc*. **2009**, *131*, 11234. (b) Canty, A. J.; Ariafard, A.; Sanford M. S.; Yates, B. F. Mechanism of Pd-Catalyzed Ar-Ar Bond Formation Involving Ligand-Directed C-H Arylation and Diaryliodonium Oxidants: Computational Studies of Orthopalladation at Binuclear Pd(II) Centers, Oxidation To Form Binuclear Palladium(III) Species, and Ar···Ar Reductive Coupling. *Organometallics*, **2013**, *32*, 544.

(11) (a) Ruyet, L.; Lapuh, M. I.; Koshti, V. S.; Földesi, T.; Jubault, P.; Poisson, T.; Novák, Z.; Besset, T. Z-Selective Pd-catalyzed 2,2,2-Trifluoroethylation of Acrylamides at Room Temperature. *Chem. Commun*., **2021**, *57*, 6241. (b) Canty,A. J.; Ariafard, A. Two-Stage Catalysis in the Pd-Catalyzed Formation of 2,2,2-Trifluoroethyl-Substituted Acrylamides: Oxidative Alkylation of Pd^{II} by an I^{III} Reagents and Roles for Acetate, Triflate, and Triflic Acid. *Organometallics*, **2022**, *41*, 293

(12) (a) Datta Chaudhuri, P.; Guo, R.; Malinakova, H. C. Formation of Benzofurans in a Stoichiometric Annulation Reaction between Stable Pallada(II)cycles and Hypervalent Vinyl- and Alkynyl(phenyl)iodonium Salts. *J. Organomet. Chem*., **2008**, *693*, 567. (b) Canty, A. J.; Ariafard, A.; Malinakova, H. C. DFT Characterisation of a $Pd^{II} \rightarrow I^{III}$ Adduct, and a Pd^{II} Complex Formed After Oxidative Alkenylation of Pd^{II} by $[Ph(alkenyl)I^{III}]^+$, in Pd-Mediated Oxidative Synthesis of Benzofurans Involving Pd^{IV}, Annulation and Chain-Walking. *Dalton Trans*. **2022**, *51*, 9377,

(13) Canty, A. J.; Rodemann, T.; Skelton, B. W.; White, A. H. Access to Alkynylpalladium(IV) and -Platinum(IV) Species, Including Triorgano(diphosphine)metal(IV) Complexes and the Structural Study of an Alkynyl(pincer)platinum(IV) Complex, Pt(O_2CAr_F)I($CCSiMe_3$)(NCN) (Ar_F – 4-$CF_3C_6H_4$, NCN = [2,6-(dimethylaminomethyl)phenyl-*N,C,N*]$^-$). *Organometallics* **2006**, *25*, 3996.

(14) See, for example: (a) Eberhard, M. R. Insights into the Heck Reaction with PCP Pincer Palladium(II) Complexes. *Org. Lett*. **2004**, *6*, 2125. (b) Bergbreiter, D. E.; Osburn, P. L. Mechanistic Studies of SCS-Pd Complexes Used in Heck Catalysis. *Adv. Synth. Catal*. **2005**, *347*, 172. (c) Sommer, W. J.; Yu, K.; Sears, J. S.; Ji, Y.; Zheng, X.; Davis, R. J.; Sherrill, C. D.; Jones, C. W.; Weck, M. Investigations into the Stability of Tethered Palladium(II) Pincer Complexes during Heck Catalysis. *Organometallics* **2005**, *24*, 4351. (d) Nilsson, P.; Wendt, O. F. Kinetic Investigation of a PC(sp^3)P Pincer Palladium(II) Complex in the Heck Reaction. *J. Organomet. Chem*. **2005**, *690*, 4197. (c) Corrêa da Costa, R.; Jurisch, M.; Gladysz, J. A. Synthesis of Fluorous Sulfur/Carbon/Sulfur Pincer Ligands and Palladium Complexes: New Catalyst Precursors for the Heck Reaction. *Inorg. Chim. Acta*, **2008**, *361*, 3205.

(15) Canty, A. J.; Ariafard, A. Concerted Oxidative Addition of Diaryliodine(III) Reagents to a Pincer-Palladium(II) Substrate: A Computational Analysis. *Organometallics* **2023**, *42*, 1900.

(16) Frisch, M. J.; Trucks, G. W.; Schlegel, H. B.; Scuseria, G. E.; Robb, M. A.; Cheeseman, J. R.; Scalmani, G.; Barone, V.; Petersson, G. A.; Nakatsuji, H.; Li, X.; Caricato, M.; Marenich, A. V.; Bloino, J.; Janesko, B. G.; Gomperts, R.; Mennucci, B.; Hratchian, H. P.; Ortiz, J. V.; Izmaylov, A. F.; Sonnenberg, J. L.; Williams-Young, D.; Ding, F.; Lipparini, F.; Egidi, F.; Goings, J.; Peng, P.; Petrone, A.; Henderson, T.; Ranasinghe, D.; Zakrzewski, V. G.; Gao, J.; Rega,N.; Zheng, G.; Liang, W.; Hada, M.; Ehara, M.; Toyota, K.; Fukuda, R.; Hasegawa, J.; Ishida, M.; Nakajima, T.; Honda, Y.; Kitao, O.; Nakai, H.; Vreven, T.; Throssell, K.; Montgomery, J. A.; Peralta, J. E.; Ogliaro, F.; Bearpark, M. J.; Heyd, J. J.; Brothers, E. N.; Kudin, K. N.; Staroverov, V. N.; Keith, T. A.; Kobayashi, R.; Normand, J.; Raghavachari, K.; Rendell, A. P.; Burant, J. C.; Iyengar, S. S.; Tomasi, J.; Cossi, M.; Millam, J. M.; M. Klene, M.; Adamo, C.; Cammi, R.; Ochterski, J. W.; Martin, R. L.; Morokuma, K.; Farkas, O.; Foresman, J. B.; Fox, D. J. *Gaussian 16, Revision A.03*, Gaussian, Inc., Wallingford CT, 2016.

(17) (a) Zhao, Y.; Truhlar, D. G. A New Local Density Functional for Main Group Thermochemistry, Transition Metal Bonding, Thermochemical Kinetics, and Noncovalent Interactions. *J. Chem. Phys*., **2006**, *125*, 194101. (b) Zhao, Y.; Truhlar, D. G. Density Functionals with Broad Applicability in Chemistry. *Acc. Chem. Res.*, **2008**, *41*, 157-167.

(18) Marenich, A. V.; Cramer, C. T.; Truhlar, D. G. Universal Solvation Model Based on Solute Electron Density and on a Continuum Model of the Solvent Defined by the Bulk Dielectric Constant and Atomic Surface Tensions. *J. Phys. Chem. B*, **2009**, *113*, 6378-6396.

(19) Bergner, A.; Dolg, M.; Küchle, W.; Stoll, H.; Preuß, H. Ab Initio Energy-Adjusted Pseudopotentials for Elements of Groups 13-17. *Mol. Phys.*, **1993**, *80,* 6, 1431-1441.

(20) (a) Ehrlich, S.; Moellmann, J.; Grimme, S. Dispersion-Corrected Density Functional Theory for Aromatic Interactions in Complex Systems. *Acc. Chem. Res*., **2013**, *46*, 916. (b) Antony, J.; Sure , R.; Grimme, S. Using Dispersion-Corrected Density Functional Theory to Understand Supramolecular Binding Thermodynamics. *Chem. Commun*., **2015**, *51*, 1764.

(21) Weigend, F.; Furche, F.; Ahlrichs, R. Gaussian Basis Sets of Quadruple Zeta Valence Quality for Atoms H-Kr. *J. Chem. Phys.*, **2003**, *119*, 12753-12762.

(22) (a) Kelly, C. P.; Cramer, C. G.; Truhlar, D. G. Aqueous Solvation Free Energies of Ions and Ion-Water Clusters Based on an Accurate Value for the Absolute Aqueous Solvation Free Energy of the Proton. *J. Phys. Chem. B*, **2006**, *110*, 16066-16081. (b) Kelly, C. P.; Cramer, C. J. Single-Ion Solvation Free Energies and the Normal Hydrogen Electrode Potential in Methanol, Acetonitrile, and Dimethyl Sulfoxide. *J. Phys. Chem. B*, **2007**, *111*, 408-422.

(23) Upon suggestion by a reviewer, we also explored the possibility of formation of a transition state commencing from a model with *mer*-NCN-coordination and the bicarbonate donor present as a monodentate [OBz···$HOCO_2$-*O*]$^-$. Optimization led to a transition state in which one N-donor arm is dissociated from palladium, analogous to structures presented in Scheme 2, and a high barrier for formation of the desired alkene product ($\Delta G^{\ddagger}$ 45 7 kcal/mol).

(24) Louie, J.; Hartwig, J. F. A Route to Pd^0 from Metallacycles in Amination and Cross-Coupling Chemistry. *Angew. Chem. Int. Ed. Engl.* **1996**, *35*, 2359.

(25) Negishi, E.-I. Ch. I.2, *Handbook of Organopalladium Chemistry for Organic Synthesis*, Vol. 1.

(26) For an example of a similar deprotonation process, in which deprotonation of the methylene group of glycine coordinated to Au^{III} is facilitated by water bridging between the methylene group and a chloride ligand, see Chipman, A.; Gouranourimi, A.; Farshadfar, K.; Olding, A.; Yates, B. F.; Ariafard, A. A Computational Mechanistic Investigation into Reduction of Gold(III) Complexes by Amino Acid Glycine: A New Variant for Amine Oxidation. *Chem. Eur. J.* **2018**, *24*, 8361.

(27) (a) von Schenck, H.; Åkermark, B.; Svensson, M. *Organometallics* **2002**, *21*, 2248. (b) von Schenck, H.; Åkermark, B.; Svensson, M. Electronic Control of the Regiochemistry in the Heck Reaction. *J. Am. Chem. Soc.* **2003**, *125*, 3503. (c) Balcells, D.; Maseras, F.; Keay, B. A.; Ziegler, T. Polyene Cyclization by a Double Intramolecular Heck Reaction. A DFT Study. *Organometallics* **2004**, *23*, 2784. (d) Surawatanawong, P.; Hall, M. B. Theoretical Study of Alternative Pathways for the Heck Reaction through Dipalladium and "Ligand-Free" Palladium Intermediates. *Organometallics* **2008**, *27*, 6222.

Table of Contents Entry